Co-ordination chemistry and molecular mechanics study of the magnesium(II) and calcium(II) complexes of trisubstituted 1,4,7-triazacyclononane derivatives

Jurriaan Huskens[a] and A. Dean Sherry *,†,a,b

[a] University of Texas at Dallas, Department of Chemistry, PO Box 830688, Richardson, Texas 75083-0688, USA
[b] University of Texas Southwestern Medical Center, Department of Radiology, the Rogers Magnetic Resonance Center, 5801 Forest Park Road, Dallas, Texas 75235-9085, USA

The affinities of 1,4,7-tris(2-hydroxyalkyl)-1,4,7-triazacyclononane derivatives for Mg^{II} and Ca^{II} were found to differ greatly. Whereas 1,4,7-tris(2-hydroxyethyl)- (L^1), 1,4,7-tris(2-hydroxy-2-methylpropyl)- (L^2) and the unsymmetrical 1,4,7-tris(2-hydroxypropyl)-1,4,7-triazacyclononane derivative L^{3b} barely discriminated between Mg^{II} and Ca^{II}, the symmetrical isomer L^{3a} was more than 500 times more selective for Mg^{II} than for Ca^{II}. Similar selectivity differences were observed between the diastereomers of 1,4,7-tris(2-hydroxy-2-phenylethyl)- (L^4) and 1,4,7-tris(2-hydroxydodecyl)-1,4,7-triazacyclononane (L^5). These selectivities were related to the structure of the magnesium complexes as shown by molecular mechanics (MMX) calculations. Only those ligands favoring the formation of a magnesium complex with a large twist angle between the planes of co-ordinating oxygens and ring nitrogens resulting in a small, tight cavity showed a large preference for Mg^{II} over Ca^{II}. The MMX calculations predicted large twist angle structures for phosphinate derivatives, and for a phosphonate monoester derivative, and these ligands were found to have a high selectivity for Mg^{II}. Similarly, the calculated preference for the smaller twist angle correctly predicted the lack of Mg^{II}/Ca^{II} selectivity for acetate and amide derivatives and for a phosphonate diester derivative. Equilibration of the complexes of the ligands in the presence of both Mg^{II} and Ca^{II} was slow, as shown for example by $k_{d,0} = 2.1 \times 10^{-4}$ s^{-1} for CaL^{3a}. These dissociation rates were a factor of 100 times larger at the boundary of a two-phase (water–chloroform) system.

In the development of ligand systems for the assessment of free, ionized magnesium(II) in biological systems, the binding selectivity for Mg^{II} over Ca^{II} is of utmost importance. Generally, ligands bind Ca^{II} preferentially due to the lower charge density and, consequently, smaller solvation heats for this ion compared to the smaller Mg^{II}.[1] As observed before,[2] 1,4,7-triazacyclononane derivatives are especially promising because they provide a small cavity and can saturate the first co-ordination sphere of Mg^{II}. Recently, we described several 1,4,7-triazacyclononane [9]aneN$_3$ derivatives that showed a selectivity for Mg^{II} over Ca^{II} of, in some cases, more than two orders of magnitude.[3–5] Although this macrocyclic structure guarantees a higher Mg^{II}/Ca^{II} selectivity ($K_{sel} = K_{MgL}/K_{CaL}$) over most other ligand systems,[2] there are significant selectivity differences between 1,4,7-triazacyclononane derivatives. 1,4,7-Triazacyclononane-1,4,7-triacetate (nota), for example,[6] has a K_{sel} of only 5.9 while for 1,4,7-triazacyclononane-1,4,7-triyltrimethylene tris(methylphosphinate), $K_{sel} = 170$.[5]

This study extends the material presented before in a preliminary communication[7] in which we discussed some remarkable selectivity differences between 1,4,7-tris(2-hydroxyalkyl)-1,4,7-triazacyclononane derivatives. Here, we report the preparation and selectivity studies of these and several other [9]aneN$_3$ derivatives with amide, phosphinate ester, and phosphonate mono- and di-ester side-chains. These selectivity differences observed by ^{13}C NMR spectroscopy are correlated to structural differences between the complexes of Mg^{II} and Ca^{II}, as predicted by molecular mechanics. Kinetic details on complexation equilibria are also provided.

† E-Mail: sherry@utdallas.edu

Experimental

General

All chemicals were purchased from Aldrich and used as received. Proton (500 MHz) and ^{13}C (125 MHz) NMR spectra were recorded at 298 K on a General Electric GN500 spectrometer using a 5 mm $^{13}C/^1H$ probe. Deuteriated acetonitrile was used as a (co-)solvent; residual CHD_2CN was used as the ^1H internal chemical shift standard (δ 1.93), while the CD_3 resonance (δ 1.3) was used as a reference for the ^{13}C chemical shifts. Although proton decoupling was usually applied, coupled spectra were recorded occasionally for assignment purposes. Resonance areas were determined by peak integration using standard GE software. No corrections for differences in nuclear Overhauser effects (NOEs) or T_1 relaxation rates were made since it was shown in a previous study[5] that these did not change upon complexation with Mg^{II}. Typically, samples contained 0.2 M ligand and magnesium or calcium perchlorate was added in aliquots of 0.25 equivalent to yield concentrations of 0–0.3 M. In the selectivity experiments (see below), 1.5 equivalents of $Mg(ClO_4)_2$ were added to the CaL sample and $Ca(ClO_4)_2$ to the MgL sample. Both were monitored as a function of time until equilibrium was reached. In a few cases, the amount of Ca^{II} was increased further to 30 equivalents in order to obtain an accurate selectivity value.

The dissociation rates of MgL^5 and MgL^8 at a $CDCl_3$–water bilayer were determined as follows. The complex (5 cm^3, 40 mM) was prepared in $CDCl_3$ and was brought into contact with an aqueous solution (5 cm^3, 10% D_2O) containing 40 mM ethylenedinitrilotetraacetate (edta), buffered with 80 mM $NaHCO_3$ and additional NaOH to pH 7.0. These systems were

stirred vigorously and 0.5 cm³ samples were collected from both phases after 5, 15, 30 min, 1 and 3 h. The organic phase samples were studied by ^{13}C NMR spectroscopy, using CDCl₃ as the internal standard (δ 77.0), while Bu^{t}OH was added to the aqueous samples as an internal standard (CH₃, δ 31.2).

Synthesis of the ligands

1,4,7-Tris(2-hydroxyethyl)-1,4,7-triazacyclononane L¹. All tris(2-hydroxyalkyl) derivatives were prepared by the reaction of [9]aneN₃ with the corresponding epoxide, using a procedure similar to that described previously.[8] Compound L¹ was prepared using [9]aneN₃ (263 mg, 2.04 mmol) and ethylene oxide (280 mg, 6.36 mmol) in water (3 cm³) at 0 °C. The temperature was gradually raised to 25 °C. After 1 h the solvent was evaporated and the residue dissolved in an equimolar mixture of diethyl ether and CH₂Cl₂. The solution was dried over Na₂SO₄, filtered, and evaporated yielding 412 mg (1.58 mmol, 77%) of L¹ isolated as a white solid, judged pure by ^{1}H and ^{13}C NMR spectroscopy. ^{1}H NMR (CD₃CN): L¹, δ 4.86 (3 H, OH, s), 3.45 (6 H, CH₂C*H₂*OH, t, $^3J_{HH}$ = 5.5 Hz), 2.64 (6 H, C*H₂*CH₂OH, t) and 2.58 (12 H, ring CH₂, s); MgL¹, δ 6.64 (3 H, OH, s), 3.88 (6 H, CH₂C*H₂*OH, t, $^3J_{HH}$ = 6.1 Hz), 3.00 (6 H, C*H₂*CH₂OH, t) and 2.97–2.73 (12 H, ring CH₂, m); CaL¹, δ 5.06 (3 H, OH, s), 3.76 (6 H, CH₂C*H₂*OH, t, $^3J_{HH}$ = 5.3 Hz), 2.77 (6 H, C*H₂*CH₂OH, t) and 2.80–2.69 (12 H, ring CH₂, m). ^{13}C NMR (CD₃CN): L¹, δ 60.78, 60.21 (CH₂CH₂OH) and 54.63 (ring CH₂); MgL¹, δ 60.50, 58.71 (CH₂CH₂OH) and 53.90 (ring CH₂); CaL¹, δ 59.64, 59.48 (CH₂CH₂OH) and 52.73 (ring CH₂).

1,4,7-Tris(2-hydroxy-2-methylpropyl)-1,4,7-triazacyclononane L². Compound L² was prepared from [9]aneN₃ (245 mg, 1.90 mmol) and isobutylene oxide (2,2-dimethyloxirane) (557 mg, 7.74 mmol) in water (3 cm³) at 25 °C. After 15 h the mixture was evaporated and dried in high vacuum yielding 576 mg (1.67 mmol, 88%) of L² isolated as a white solid, judged pure by ^{1}H and ^{13}C NMR spectroscopy. ^{1}H NMR (CD₃CN–CDCl₃, 3:1 v/v): L², δ 3.89 (3 H, OH, s), 2.87 [6 H, C*H₂*C(CH₃)₂OH, s], 2.47 (12 H, ring CH₂, s) and 1.08 (18 H, CH₃, s); MgL², δ 6.19 (3 H, OH, s), 2.90 [6 H, C*H₂*C(CH₃)₂OH, s], 2.84 (12 H, ring CH₂, s) and 1.38 (18 H, CH₃, s); CaL², δ 5.05 (3 H, OH, s), 2.90 [6 H, C*H₂*C(CH₃)₂OH, s], 2.72 (12 H, ring CH₂, s) and 1.31 (18 H, CH₃, s). ^{13}C NMR (CD₃CN–CDCl₃, 3:1 v/v): L², δ 72.10 [CH₂*C*(CH₃)₂OH], 70.92 [*C*(CH₃)₂OH], 61.21 (ring CH₂) and 28.45 (CH₃); MgL², δ 73.68 [*C*(CH₃)₂OH], 66.46 [*C*H₂C-(CH₃)₂OH], 53.10 (ring CH₂) and 30.67 (CH₃); CaL², δ 72.98 [*C*(CH₃)₂OH], 69.17 [*C*H₂C(CH₃)₂OH], 54.33 (ring CH₂) and 30.75 (CH₃).

1,4,7-Tris[(2S)-2-hydroxypropyl]-1,4,7-triazacyclononane L³ᵃ. Pure compound L³ᵃ was prepared similarly to that described previously,[9] from [9]aneN₃ (238 mg, 1.84 mmol) and (S)-propylene oxide (436 mg, 7.51 mmol) in chloroform (3 cm³), while warming the sample from 0 to 25 °C during the first 1 h. After 3 d the mixture was evaporated in high vacuum yielding 531 mg (1.75 mmol, 95%) of L³ᵃ isolated as a white solid, judged pure by ^{1}H and ^{13}C NMR spectroscopy. ^{1}H NMR (CD₃CN): L³ᵃ, δ 5.52 (3 H, OH, s), 3.76 (3 H, CH, m), 2.76, 2.41 (12 H, ring CH₂, two d), 2.57, 2.30 [6 H, C*H₂*CH(CH₃)OH, two dd, $^2J_{HH}$ = −13.5, $^3J_{HH}$ = 2.6, 9.5] and 0.99 (9 H, CH₃, d, $^3J_{HH}$ = 6.2 Hz); MgL³ᵃ, δ 6.52 (3 H, OH, s), 4.24 (3 H, CH, m), 2.86, 2.78 [6 H, C*H₂*CH(CH₃)OH, two dd, $^2J_{HH}$ = −15.1, $^3J_{HH}$ = 6.2, 7.0], 3.02–2.64 (12 H, ring CH₂, m) and 1.23 (9 H, CH₃, d, $^3J_{HH}$ = 6.0 Hz); CaL³ᵃ, δ 5.01 (3 H, OH, s), 4.14 (3 H, CH, m), 2.90–2.72 (12 H, ring CH₂, m), 2.66, 2.58 [6 H, C*H₂*CH(CH₃)OH, two dd, $^2J_{HH}$ = −12.2, $^3J_{HH}$ = 3.7, 8.5] and 1.17 (9 H, CH₃, d, $^3J_{HH}$ = 6.2 Hz). ^{13}C NMR (CD₃CN): L³ᵃ, δ 67.50 [*C*H₂CH(CH₃)OH], 64.48 (CH), 53.96 (ring CH₂) and 20.60 (CH₃); MgL³ᵃ, δ 68.48 [*C*H₂CH(CH₃)OH], 64.96 (CH), 57.26, 51.17 (ring CH₂) and 19.94 (CH₃); CaL³ᵃ, δ 67.34 [*C*H₂CH(CH₃)OH], 66.33 (CH), 57.00, 51.87 (ring CH₂) and 21.22 (CH₃).

1,4,7-Tris(2-hydroxypropyl)-1,4,7-triazacyclononane (L³ᵃ: L³ᵇ = 1:3). Analogous to the procedure for compound L³ᵃ, a 1:3 mixture of L³ᵃ and L³ᵇ was prepared from [9]aneN₃ (258 mg, 2.00 mmol) and racemic propylene oxide (415 mg, 7.16 mmol) yielding 555 mg (1.83 mmol, 92%) of the diastereomeric mixture, isolated as a white solid. ^{1}H NMR (CD₃CN): L³ᵇ, δ 5.22 (3 H, OH, s), 3.75 (3 H, CH, m), 2.80–2.25 [18 H, ring CH₂ and C*H₂*CH(CH₃)OH, m] and 1.00 (9 H, CH₃, m); MgL³ᵇ, δ 6.42, 6.12 [3 H, OH, two s (2:1)], 4.10 (3 H, CH, m), 3.10–2.05 [18 H, ring CH₂ and C*H₂*CH(CH₃)OH, m] and 1.20 (9 H, CH₃, m); CaL³ᵇ, δ 5.08, 4.82, 4.71 (3 H, OH, three s), 4.15 (3 H, CH, m), 2.80–2.42 [18 H, ring CH₂ and C*H₂*CH(CH₃)OH, m] and 1.17 (9 H, CH₃, m). ^{13}C NMR (CD₃CN): L³ᵇ, δ 68.41, 67.21 [1:2, *C*H₂CH(CH₃)OH], 65.36, 64.76 (1:2, CH), 55.24, 54.64, 54.39 (ring CH₂), 20.75, 20.60 (1:2, CH₃); MgL³ᵇ, δ 68.16, 67.63, 66.89 [*C*H₂CH(CH₃)OH], 66.16, 64.78, 64.34 (CH), 57.33, 55.23, 53.36, 52.51, 51.66, 50.86 (ring CH₂), 19.95, 19.54, 19.03 (CH₃); CaL³ᵇ, δ 67.48, 67.05, 66.59 [*C*H₂CH(CH₃)OH], 66.12, 65.32, 64.59 (CH), 56.34, 53.77, 53.48, 52.22, 52.00, 51.03 (ring CH₂), 21.02, 20.75 (2:1, CH₃).

1,4,7-Tris[(2S)-2-hydroxy-2-phenylethyl]-1,4,7-triazacyclononane L⁴ᵃ. Compound L⁴ᵃ was prepared from [9]aneN₃ (161 mg, 1.25 mmol) and (S)-styrene oxide (606 mg, 5.04 mmol) in chloroform (3 cm³) at 25 °C. After 2 d the solvent was evaporated and the residue dissolved in MeOH. The product was separated from excess of epoxide and an impurity (likely the adduct of an extra epoxide with L⁴ᵃ at a hydroxy site) by column chromatography (silica, using 0–10% concentrated ammonia in MeOH as the eluent). Thus, 128 mg (0.262 mmol, 21%) of L⁴ᵃ were obtained as an off-white solid, judged pure by ^{1}H and ^{13}C NMR spectroscopy. ^{1}H NMR (CD₃CN): L⁴ᵃ, δ 7.41 (6 H, o-H of Ph, d, $^3J_{HH}$ = 7.3), 7.34 (6 H, m-H of Ph, t), 7.25 (3 H, p-H of Ph, t, $^3J_{HH}$ = 7.4), 6.28 (3 H, OH, s), 4.86 (3 H, CH, dd, $^3J_{HH}$ = 2.6, 11.7), 2.95, 2.58 (12 H, ring CH₂, two d), 2.84, 2.66 [6 H, C*H₂*CH(Ph)OH, two dd, $^2J_{HH}$ = −13.0 Hz]; MgL⁴ᵃ, δ 7.54 (6 H, o-H of Ph, d, $^3J_{HH}$ = 7.4), 7.41 (6 H, m-H of Ph, t), 7.38 (3 H, p-H of Ph, t, $^3J_{HH}$ = 7.4), 7.03 (3 H, OH, s), 5.28 (3 H, CH, dd, $^3J_{HH}$ = 3.7, 12.3), 3.14, 3.06 [6 H, C*H₂*CH(Ph)OH, two dd, ^2J = −15.0 Hz], 3.26–2.95 (12 H, ring CH₂, m); CaL⁴ᵃ, δ 7.47 (6 H, o-H of Ph, d, $^3J_{HH}$ = 7.3), 7.41 (6 H, m-H of Ph, t), 7.34 (3 H, p-H of Ph, t, $^3J_{HH}$ = 7.5), 5.96 (3 H, OH, s), 5.09 (3 H, CH, dd, $^3J_{HH}$ = 3.8, 9.2), 3.04, 2.91 [6 H, C*H₂*CH(Ph)OH, two dd, $^2J_{HH}$ = −12.9 Hz], 2.93–2.63 (12 H, ring CH₂, m). ^{13}C NMR (CD₃CN): L⁴ᵃ, δ 144.11 (ipso-C), 129.10, 126.87 (o/m-C of Ph), 128.02 (p-C of Ph), 71.43 (CH), 68.17 [*C*H₂CH(Ph)OH] and 53.41 (ring CH₂); MgL⁴ᵃ, δ 138.66 (ipso-C), 129.01, 127.80 (o/m-C of Ph), 130.11 (p-C of Ph), 74.28 (CH), 65.55 [*C*H₂CH-(Ph)OH], 57.16, 51.35 (ring CH₂); CaL⁴ᵃ, δ 142.03 (ipso-C), 129.54, 126.89 (o/m-C of Ph), 129.13 (p-C of Ph), 73.06 (CH), 66.55 [*C*H₂CH(Ph)OH], 56.68, 51.89 (ring CH₂).

(±)-1,4-Bis[(2R)-2-hydroxy-2-phenylethyl]-7-[(2S)-2-hydroxy-2-phenylethyl]-1,4,7-triazacyclononane L⁴ᵇ. Analogous to the procedure for compound L⁴ᵃ, 143 mg (0.292 mmol, 15%) pure L⁴ᵇ was recovered as an off-white solid, judged pure by ^{1}H and ^{13}C NMR spectroscopy, from the reaction between [9]aneN₃ (256 mg, 1.98 mmol) and racemic styrene oxide (996 mg, 8.30 mmol). ^{1}H NMR (CD₃CN): L⁴ᵇ, δ 7.41 (6 H, o-H of Ph, d), 7.34 (6 H, m-H of Ph, t), 7.26 (3 H, p-H of Ph, t), 6.05 (3 H, OH, s), 4.83 (3 H, CH, m), 2.95–2.60 [18 H, ring CH₂ and C*H₂*CH(Ph)OH, m]; MgL⁴ᵇ, δ 7.35–7.55 (15 H, Ph, m), 7.13, 6.91, 6.86 (3 H, OH, three s), 5.20 (3 H, CH, m), 3.25–2.75 [18 H, ring CH₂ and C*H₂*CH(Ph)OH, m]; CaL⁴ᵇ, δ 7.30–7.50 (15 H, Ph, m), 5.90, 5.50, 5.39 (3 H, OH, three s), 5.09 (3 H, CH, m), 3.20–2.65 [18 H, ring CH₂ and C*H₂*CH(Ph)OH, m]. ^{13}C NMR (CD₃CN): L⁴ᵇ, δ 144.26, 144.12 (1:2, ipso-C), 129.21, 129.03, 126.97, 126.79 (o/m-C of Ph), 128.14, 127.96 (p-C of Ph), 72.08, 71.58 (1:2, CH), 69.10, 67.87 [1:2, C*H₂*CH(Ph)OH], 54.71, 54.11, 53.82 (ring CH₂); MgL⁴ᵇ, δ 138.97, 138.64, 138.36

(*ipso*-C), 130.67, 130.53, 130.48, 130.17, 129.79, 127.70 (*o*/*m*/*p*-C of Ph), 73.96, 73.60, 72.29 (CH), 66.44, 65.35, 64.24 [CH_2CH(Ph)OH], 57.18, 55.34, 53.63, 52.55, 51.74, 50.96 (ring CH_2); CaL^{4b}, δ 141.75, 141.62, 141.34 (*ipso*-C), 129.68, 129.50, 127.38, 127.27, 127.19, 127.08 (*o*/*m*/*p*-C of Ph), 73.26, 72.89, 72.43 (CH), 67.74, 65.59, 64.89 [CH_2CH(Ph)OH], 56.37, 53.69, 53.32, 52.07, 51.78, 50.88 (ring CH_2).

1,4,7-Tris(2-hydroxydodecyl)-1,4,7-triazacyclononane (L^{5a}:L^{5b} = 1:3).

A 1:3 mixture of compounds L^{5a} and L^{5b} was prepared from [9]aneN$_3$ (255 mg, 1.98 mmol) and racemic 1,2-epoxydodecane (1.684 g, 9.14 mmol) at 80 °C without additional solvent. After 15 h the mixture was evaporated in high vacuum. After addition of MeOH an oily layer separated. After evaporation in high vacuum this appeared to be 290 mg (0.426 mmol, 22%) of the pure diastereomeric mixture isolated as a waxy solid. ^{1}H NMR (CD$_3$CN–CDCl$_3$, 2:1 v/v): L^{5a}:L^{5b} 1:3, δ 5.50 (4 H, OH, s), 3.60 (4 H, CH, m), 2.80–2.30 [24 H, ring CH_2 and CH_2CH(OH)R, m], 1.90 (8 H, m), 1.40–1.10 (64 H, m) and 0.85 (12 H, t) (C$_{10}$H$_{21}$); MgL^{5a} and MgL^{5b}, δ 6.13, 6.07, 5.88, 5.81 (4 H, OH, s), 4.05 (4 H, CH, m), 3.10–2.55 [24 H, ring CH_2 and CH_2CH(OH)R, m], 1.50–1.20 (72 H, m) and 0.85 (12 H, t) (C$_{10}$H$_{21}$); CaL^{5a} and CaL^{5b}, δ 4.87, 4.84, 4.65, 4.53 (4 H, OH, s), 3.95 (4 H, CH, m), 3.00–2.45 [24 H, ring CH_2 and CH_2CH(OH)R, m], 1.50–1.20 (72 H, m) and 0.85 (12 H, t) (C$_{10}$H$_{21}$). ^{13}C NMR (CD$_3$CN–CDCl$_3$, 2:1 v/v): L^{5a} (*) and L^{5b}, δ 69.10, 68.40,* 67.98 [1:2:1, CH$_2$CH(C$_{10}$H$_{21}$)OH], 66.85, 65.85, 65.66* (1:1:2, CH), 54.84, 54.27, 53.99, 53.39* (ring CH_2), 35.53, 35.45* (1:3, CHOHCH_2CH$_2$R), 26.22 (CHOHCH$_2$-CH_2R), 32.39, 30.24, 30.11, 29.82, 23.13, 14.35 (CHOHCH$_2$-CH$_2$*R*); MgL^{5a} (*) and MgL^{5b}, δ 72.08,* 71.76, 71.36, 70.61 [CH_2CH(OH)R], 64.60, 63.31,* 63.13, 62.87 (CH), 57.02, 56.76,* 55.07, 53.38, 52.48, 51.49, 50.95,* 50.73 (ring CH_2), 34.82,* 34.60, 34.28, 34.06 (CHOHCH_2CH$_2$R), 25.30, 25.10, 25.00, 24.75 (CHOHCH$_2$$CH_2$R), 32.34, 30.05, 30.01, 29.92, 29.79, 23.11, 14.32 (CHOHCH$_2$CH$_2$*R*); CaL^{5a} (*) and CaL^{5b}, δ 71.13,* 70.62, 70.23, 69.61 [CH_2CH(OH)R], 65.65, 64.56,* 63.37, 62.76 (CH), 56.70,* 56.22, 53.58, 53.15, 51.88, 51.77, 51.62,* 50.75 (ring CH_2), 35.78,* 35.69, 35.38 (1:2:1, CHOH-CH_2CH$_2$R), 25.59, 25.40, 25.25 (1:2:1, CHOHCH$_2$$CH_2$R), 32.39, 30.08, 29.83, 23.15, 14.34 (CHOHCH$_2$CH$_2$*R*).

1,4,7-Tris(diethylcarbamoylmethyl)-1,4,7-triazacyclononane L^6.

The compound [9]aneN$_3$ (254 mg, 1.97 mmol), 2-chloro-*N,N*-diethylacetamide (1.070 g, 7.15 mmol) and NaHCO$_3$ (675 mg, 8.04 mmol) were refluxed in MeOH (10 cm^3) under N$_2$, similarly as described before for the analogous 1,4,7,10-tetraazacyclododecane derivative.[10] After 4 h the mixture was cooled to room temperature, NaHCO$_3$ and NaCl were filtered off, and the solvent was evaporated yielding 1.358 g of the crude product. The residue was dissolved in water and washed with diethyl ether thus removing excess alkylating agent. The product was extracted into CH$_2$Cl$_2$, which was dried over Na$_2$SO$_4$. After filtration and evaporation, 500 mg (1.07 mmol, 54%) of L^6 were recovered as a clear oil, judged pure by ^{1}H and ^{13}C NMR spectroscopy. ^{1}H NMR (CD$_3$CN): L^6, δ 3.36 (6 H, CH$_2$CO, s), 3.36, 3.27 (12 H, CH_2CH$_3$, two q, $^3J_{HH}$ = 7.0 Hz), 2.80 (12 H, ring CH_2, s), 1.11, 1.02 (18 H, CH$_3$, two t); MgL^6, δ 3.81 (6 H, CH$_2$CO, s), 3.42, 3.33 (12 H, CH_2CH$_3$, two q, $^3J_{HH}$ = 7.0 Hz), 2.90, 2.68 (12 H, ring CH_2, m), 1.15, 1.11 (18 H, CH$_3$, two t); CaL^6, lines too broad to assign. ^{13}C NMR (CD$_3$CN): L^6, δ 170.17 (CO), 60.22 (CH$_2$CO), 55.68 (ring CH_2), 41.92, 40.25 (CH$_2$CH$_3$), 14.52, 13.30 (CH$_3$); MgL^6, δ 173.52 (CO), 58.59 (CH$_2$CO), 52.01 (ring CH_2), 43.13, 42.95 (CH$_2$CH$_3$), 13.88, 12.70 (CH$_3$); CaL^6, δ 172.95 (CO), 61.18 (CH$_2$CO), 53.74 (ring CH_2), 43.15, 42.44 (CH$_2$CH$_3$), 14.40, 13.16 (CH$_3$).

1,4,7-Triazacyclononane-1,4,7-triyltrimethylenetris(methylphosphinic acid ethyl ester) L^7.

The triethyl ester L^7 was pre-pared as described before (this study also includes ^{1}H NMR data).[5] ^{13}C NMR (CD$_3$CN–CDCl$_3$, 1:1 v/v): L^7, δ 60.42 (OCH$_2$, $^2J_{PC}$ = 6.1), 58.09 (NCH$_2$P, $^1J_{PC}$ = 114), 58.08 (ring CH$_2$), 16.90 (OCH$_2$CH$_3$) and 13.40 (PCH$_3$, $^1J_{PC}$ = 90.5 Hz); MgL^7, δ 64.52 ($^2J_{PC}$ = 6.6), 64.29 and 64.13 ($^2J_{PC}$ = 8.5) (1:2:1, OCH$_2$), 58.0–54.0 (ring CH$_2$ and NCH$_2$P), 16.47, 16.40, 16.32 (2:1:1, OCH$_2$CH$_3$), 13.94 ($^1J_{PC}$ = 95.9), 13.68 ($^1J_{PC}$ = 94.5) and 13.43 ($^1J_{PC}$ = 90.0 Hz) (1:2:1, PCH$_3$); CaL^7, δ 62.91 (OCH$_2$, br), 54.2–59.5 (ring CH$_2$ and NCH$_2$P), 16.51, 16.43 (2:2, OCH$_2$CH$_3$), 14.06 ($^1J_{PC}$ = 86.3), 13.58 ($^1J_{PC}$ = 91.7), 13.37 ($^1J_{PC}$ = 87.6) and 13.13 ($^1J_{PC}$ = 89.6 Hz) (PCH$_3$).

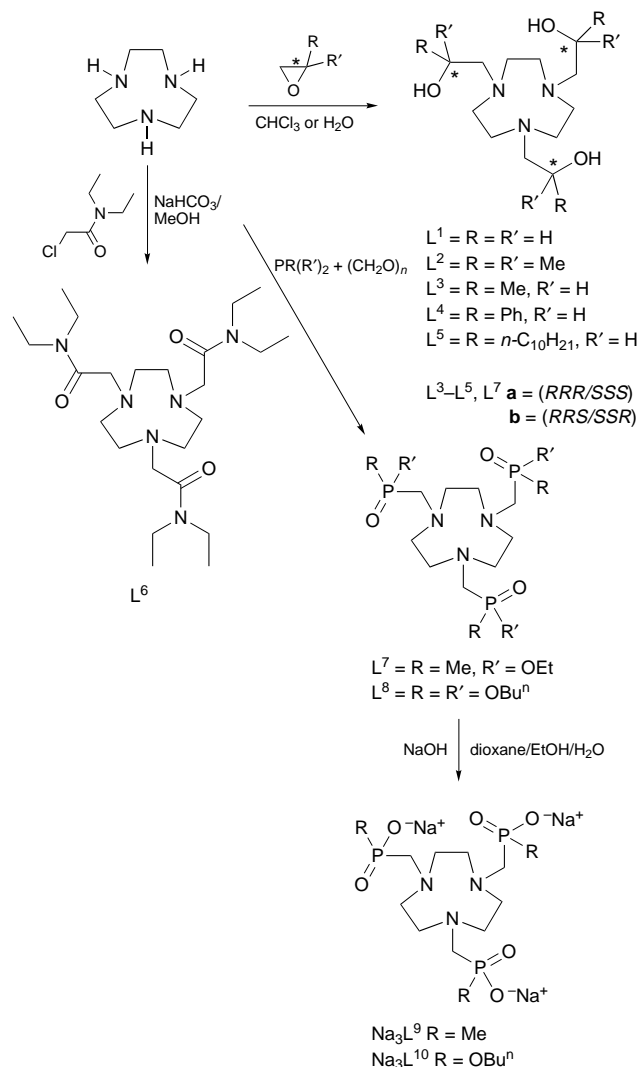### 1,4,7-Triazacyclononane-1,4,7-triyltrimethylenetris(phosphonic acid dibutyl ester) L^8.

The compound [9]aneN$_3$ (247 mg, 1.91 mmol), (CH$_2$O)$_n$ (178 mg, 5.94 mmol) and P(OBu^n)$_3$ (1.580 g, 6.32 mmol) were mixed at 25 °C without any additional solvent. After 15 h the mixture was evaporated in high vacuum, yielding 1.558 g of L^8, judged >90% pure by ^{13}C NMR spectroscopy, which was used without further purification. ^{13}C NMR (CD$_3$CN): L^8, δ 65.98 (OCH$_2$, $^2J_{PC}$ = 6.4), 57.53 (ring CH$_2$, $^3J_{PC}$ = 5.7), 53.98 (NCH$_2$P, $^1J_{PC}$ = 160 Hz), 33.39 (OCH$_2$CH$_2$), 19.51 (CH$_2$CH$_3$) and 13.94 (CH$_3$); MgL^8, δ 70.01 (OCH$_2$, $^2J_{PC}$ = 5.9), 55.35 (ring CH$_2$, $^3J_{PC}$ = 8.3), 54.11 (NCH$_2$P, $^1J_{PC}$ = 151 Hz), 32.69 (OCH$_2$CH$_2$), 19.19 (CH$_2$CH$_3$) and 13.77 (CH$_3$); CaL^8, δ 68.42 (OCH$_2$, $^2J_{PC}$ = 6.8), 55.20 (ring CH$_2$, $^3J_{PC}$ = 7.0), 54.38 (NCH$_2$P, $^1J_{PC}$ = 156 Hz), 32.86 (OCH$_2$CH$_2$), 19.29 (CH$_2$CH$_3$) and 13.83 (CH$_3$).

Trisodium 1,4,7-triazacyclononane-1,4,7-triyltrimethylene tris(phosphonate monobutyl ester) Na$_3$L^{10}.

Compound L^8 (750 mg, 0.92 mmol) was refluxed in a mixture of water (10 cm^3), 1,4-dioxane (10 cm^3), EtOH (5 cm^3) and 40% aqueous NaOH (5 cm^3) for 2 d. After evaporation, a concentrated aqueous phase and a gummy residue were obtained. The aqueous phase was decanted and the residue dissolved in CH$_2$Cl$_2$, which was dried over Na$_2$SO$_4$. After filtration and evaporation, 392 mg (0.62 mmol, 68%) of L^{10} (trisodium salt) was obtained, judged >90% pure by ^{13}C NMR spectroscopy, which was used without further purification. ^{13}C NMR (CD$_3$CN–CDCl$_3$, 1:1 v/v): L^{10}, δ 64.57 (OCH$_2$, br), 54.47 (ring CH$_2$, br), 56.30 (NCH$_2$P, $^1J_{PC}$ = 149 Hz), 33.49 (OCH$_2$CH$_2$), 19.42 (CH$_2$CH$_3$) and 14.12 (CH$_3$); MgL^{10}, δ 64.84 (OCH$_2$, $^2J_{PC}$ = 4.1), 58.47 ($^3J_{PC}$ = 8.3) and 52.90 (ring CH$_2$), 56.59 (NCH$_2$P, $^1J_{PC}$ = 148), 33.33 (OCH$_2$CH$_2$, $^3J_{PC}$ = 5.4 Hz), 19.36 (CH$_2$CH$_3$) and 14.07 (CH$_3$); CaL^{10}, δ 65.65 (OCH$_2$, br), 56.13 (ring CH$_2$ and NCH$_2$P, br), 33.31 (OCH$_2$CH$_2$), 19.45 (CH$_2$CH$_3$) and 14.09 (CH$_3$).

Molecular mechanics calculations

The geometries of the magnesium and calcium complexes of compounds L^1, L^2, L^{3a}, L^{3b}, nota, L^{7a}, L^{7b}, notpde (L$^{8'}$, R = R′ = OEt), L^9 and notpme (L$^{10'}$, R = OEt) were optimized using the MMX force field of HYPERCHEM 4.5 on a 486DX, 66 MHz personal computer. The built-in force field parameters for Mg^{II} and Ca^{II} were used as such. Side-chains were positioned roughly into modes A, B or C (Scheme 3) before optimization, and the positions of the OH protons in L^1–L^3, and of the residual alkyl groups in L^3, L^7–L^{10} were varied systematically for observation of local energy minima. Since it was more practical to keep the 1,4,7-triazacyclononane ring fixed in a single conformation (Δ), all statistical possibilities for the stereocenters present in the side-chains or occurring after complexation on the phosphorus or co-ordinating oxygen nuclei were investigated. For nota, only local minima with all acetates in either A or C were observed. The side-chain orientations of the structures with the lowest energy are reported in Table 2. The energy values given in Table 2 are those directly obtained from the molecular mechanics calculations.
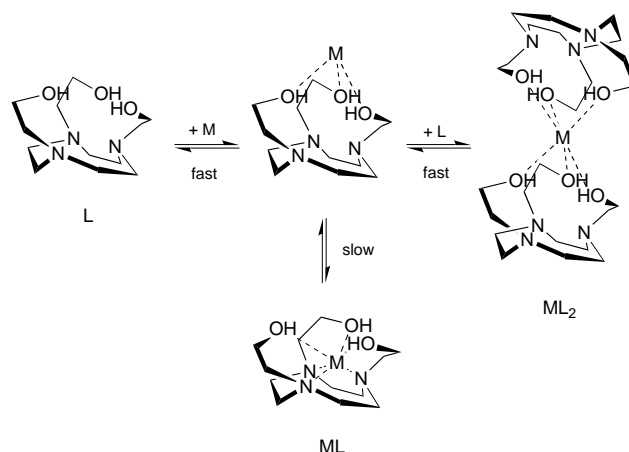
Scheme 2 Species observed in solution for MgL[1] and CaL[1], and the rates of their equilibria relative to the NMR time-scale

Scheme 1

Results and Discussion

Binding selectivities for Mg[II] versus Ca[II]

All tris(2-hydroxyalkyl) derivatives L[1]–L[5] were prepared by the reaction of 1,4,7-triazacyclononane with an excess of the corresponding epoxide (Scheme 1), as described for L[1] and L[3a].[8,9] If R ≠ R′, two diastereomers of each derivative were formed when racemic epoxide was used. The ratio between the (*RRR/SSS*) (**a**) and the (*RRS/SSR*) (**b**) forms of L[3]–L[5] was in all cases 1 : 3, as statistically expected. Optically pure L[3a] and L[4a] were prepared from the corresponding chiral (*S*)-epoxides. We were able to isolate pure L[4b] from the reaction mixture of L[4a] and L[4b] by column chromatography. The diastereomeric mixtures of L[3a] and L[3b] and of L[5a] and L[5b] were used without further separation in the selectivity experiments described below.

The tris(*N*,*N*-diethylamide) derivative of nota, L[6] (Scheme 1), was prepared analogously to the corresponding tetrasubstituted 1,4,7,10-tetraazacyclododecane derivative.[10] The phosphorus derivatives L[7] and L[8] were prepared from the corresponding phosphine and paraformaldehyde (Scheme 1), as described before for the synthesis of L[9].[5] The trisodium salt of L[10] was prepared by the hydrolysis of L[8], using an excess of NaOH (Scheme 1).

All ligands and their magnesium and calcium complexes were studied by ^{1}H and ^{13}C NMR spectroscopy at room temperature using CD_3CN as the solvent. This solvent provided good solubility for most of the ligands (for a few, additional CDCl_3 was added) and of magnesium and calcium perchlorates. Since the ^{1}H resonances of the complexes appeared to overlap consider-

ably, attention was focused mainly on the ^{13}C NMR experiments.

The ^{13}C NMR spectra of compounds L[1], L[2], L[3] and L[4a] showed single sharp resonances for the ring carbons, and for all side-chain nuclei. The unsymmetrical isomer L[4b], however, showed three separate ring resonances and three resonances for each side-chain nucleus, of which some were overlapping. Consequently, the diastereomeric mixtures of L[3a] and L[3b] and of L[5a] and L[5b] showed four resonances for the ring carbons which had equal intensity since the single line for L[3a] corresponded to six nuclei while the three lines for the more abundant (3×) isomer L[3b] corresponded to two nuclei each. The amide derivative, L[6], showed a single sharp resonance for ring carbons, but two lines for each of the ethyl nuclei due to slow rotation around the amide bond. The phosphorylated compounds L[7] and L[8] showed similar behavior, although ^{31}P couplings complicated the spectra. For L[10], broader lines were observed, especially for the ring nuclei.

Upon addition of small amounts of Mg(ClO_4)_2 the resonances of L[1]–L[6] started to shift considerably, while also a separate set of resonances appeared. The latter set appeared to be the 1 : 1 complex, ML, as it was the only species present when 1 equivalent or more of the metal ion was added to the ligand solution. This 1 : 1 complex was attributed to an inner-cage complex in which all ring nitrogens are involved in co-ordination and, likely, all three side-chain oxygens. The shift of the ligand resonances at lower metal-to-ligand ratios can probably be attributed to fast exchange species in which only the oxygens are involved in metal co-ordination (see Scheme 2). For L[7] and L[8], no shift of the free ligand resonances was observed, only the formation of the (slow-exchange) 1 : 1 complexes. For L[10], line broadening was so severe that only the spectra at excess of metal were useful.

For ML[1] and ML[2], single resonances were observed for all ring carbons and for all equivalent nuclei from the side-chains, while for ML[3a] and ML[4a] the ring carbons showed two resonances upon metal complexation. The latter can be attributed to restriction of the side-chain rotation upon formation of the co-ordinative chelate rings: the R groups then point preferentially to one side of the chelate ring which renders the two ring carbons attached to the nitrogen non-equivalent. Consequently, all six ring carbons of ML[4b] showed separate resonances, while for the diastereomeric mixtures of L[3] and L[5] eight ring carbon resonances were detected for both MgL and CaL: two arose from the symmetrical (*RRR/SSS*) isomer, while six belonged to the unsymmetrical (*RRS/SSR*) isomer. Similar to those of the free ligands, these lines had equal intensity. Analogously, the resonances of the side-chain nuclei appeared as four equally intense lines. For L[5a] and L[5b] the two carbons of the residual C_{10}H_{21} closest to the CHOH group were thus resolved into four

Table 1 Selectivities, K_{sel} ($= K_{MgL}/K_{CaL}$), of the macrocyclic ligands (Scheme 1) as obtained from ^{13}C NMR competition experiments, preferred side-chain co-ordination modes (Scheme 3) as obtained from MMX calculations (Table 2), and indications of the dissociation rates of the complexes

| | | Structure | | | | |
| | | MgL | | CaL | | |
L	K_{sel}	Mode	α/°	Mode	α/°	Dissociation[a]
L^1	0.18	BBB	14	BBB	9	Slow
L^2	3.0	BBB/CCC	21/−33	BBB	18	Slow
L^{3a}	590	AAA	36	BBB	9	Slow
L^{3b}	0.25	ABB		ABB		Slow
L^{4a}	16					Slow
L^{4b}	0.06					Slow
L^{5a}	>60^b					Slow
L^{5b}	0.28					Slow
nota	5.9^c	CCC	−27	CCC	−21	
L^6	8.8					Slow
L^{7c}	>25^b	AAA/CCC	53/−45	BBB	7	Fast
L^{7b}	>25^b	AAA/CCC		BBB		Fast
L^8	1.6	CCC	−46	BBB	12	Fast
L^9	170^d	AAA	55	BBB	14	
L^{10}	>25	AAA/CCC	53/−45	BBB	14	Slow

^{a} In organic solvent; slow, $t_{\frac{1}{2}} = 1$–8 h; fast, $t_{\frac{1}{2}} < 5$ min. ^{b} Observed only for the diastereomeric mixture. ^{c} In aqueous solution, ref. 6. ^{d} In aqueous solution, ref. 5.
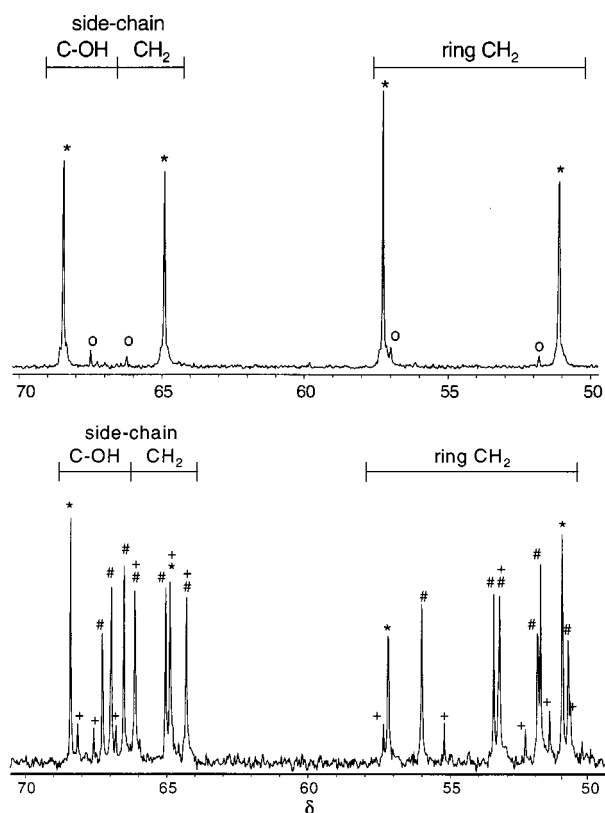
Fig. 1 The ^{13}C NMR spectrum of a sample with L^{3a} : L^{3b} : Mg : Ca = 1 : 3 : 6 : 6 (bottom) and of a sample with L^{3a} : Mg : Ca = 2 : 3 : 50; *, MgL^{3a}; o, CaL^{3a}; +, MgL^{3b}; #, CaL^{3b} (methyl resonances not shown)

lines. whereas the remaining nuclei appeared as partly overlapping, single lines. Identification of the diastereomers of L^3 and their complexes was accomplished by comparison with the spectra of optically pure L^{3a}, while for L^5 the spectra were compared to the data obtained for L^3. Similar observations were made for L^6–L^8. For L^{10} the resonances of the magnesium complex were sharp and well resolved, while the calcium complex showed considerable line broadening.

The Mg^{II}/Ca^{II} selectivities of the ligands were determined by ^{13}C NMR spectroscopy on samples with both Mg^{II} and Ca^{II} in excess, prepared by adding Mg^{II} to the sample containing CaL and by adding Ca^{II} to the MgL sample. Chemical equilibrium was assumed when both samples indicated the same metal-ion selectivity value. For a sample containing L^{3a} : L^{3b} : Mg^{II} : Ca^{II} = 1 : 3 : 6 : 6, the ^{13}C NMR spectrum (Fig. 1, bottom) showed that both Mg^{II} and Ca^{II} formed complexes with L^{3b} ($K_{sel} = 0.25$), while L^{3a} only bound Mg^{II}. Selectivity experiments with pure L^{3a} (Fig. 1, top) indicated that $K_{sel} = 590$ for this ligand. This led to the conclusion that the difference in orientation of a single methyl group in these ligands results in a Mg^{II}/Ca^{II} selectivity difference of more than three orders of magnitude. For the tris(2-hydroxyalkyl) derivatives, only L^{3a}, L^{4a} and L^{5a} exhibited large selectivities for Mg^{II} (Table 1), while L^1, L^2, L^{3b}, L^{4b} and L^{5b} barely discriminated between Mg^{II} and Ca^{II}. The amide derivative L^6, prepared earlier and tested as a carrier for alkali- and alkaline-earth-metal ions,[11] showed a low selectivity, comparable to the selectivity of nota as observed in aqueous solution.[6] The triethyl ester L^7 showed a good selectivity for Mg^{II} for both diastereomers, as shown from an absence of the calcium complex for a sample containing L^{7a} : L^{7b} : Mg^{II} : Ca^{II} = 1 : 3 : 6 : 6. The same was observed for L^{10}, but the tris-(phosphonate diester) derivative L^8 showed no selectivity at all. It should be noted that L^{10} might form diastereomeric complexes in solution since the oxygens in a phosphonate side-chain will become inequivalent upon complexation of one of them, as described for L^9.[5] The observation of a single sharp set of resonances for MgL^{10}, indicating C_3 symmetry, seems to suggest only one isomer in solution, whereas the calcium complex, exhibiting considerable line broadening, might be present as a mixture of isomers. This contrasts with the behavior of L^9 in aqueous solution, where the ^{31}P resonance for the magnesium complex was broader than for the free ligand. This was attributed to the presence of both diastereomeric complexes in solution.[5]

Structure of the complexes of Mg^{II} and Ca^{II}

To investigate further the striking selectivity differences between very closely related compounds such as L^{3a} and L^{3b}, we used molecular mechanics calculations to find the optimum structures of the magnesium and calcium complexes of L^1, L^2, L^{3a}, L^{3b}, nota, L^{7a}, L^{7b}, notpde (L$^{8\prime}$, R = R$^\prime$ = OEt), L^9 and notpme (L$^{10\prime}$, R = OEt). Local energy minima were observed for structures in which the side-chains adopted one of three possible co-ordination modes (Scheme 3), and the occurrence of these minima was attributed to a (low-energy) staggered conformation of the C–C bond in the side-chains for all co-

Table 2 Local energy minima (in kcal mol⁻¹, *ca.* 4.184 kJ mol⁻¹; n.m. = no minimum observed; lowest per complex italicized) of the macrocyclic ligand complexes of Mg^{II} and Ca^{II} as a function of the orientation of the side-chains (Scheme 3; macrocyclic ring in Δ conformation), as determined by MMX calculations

L	MgL			CaL		
	AAA	BBB	CCC	AAA	BBB	CCC
L¹ᵃ	42.30, 43.08	*41.96*, 43.79	46.58, 46.72	37.78, 38.27	36.90, *36.13*	n.m., n.m.
L²ᵃ	68.33, 65.54	65.79, *63.54*	63.64, 66.58	n.m., 61.83	56.64, *54.81*	59.35, 63.29
RRR-L³ᵃ ᵃ	61.06, n.m.	44.87, 46.29	54.03, 46.85	51.44, 51.74	40.43, *39.24*	53.32, n.m.
SSS-L³ᵃ ᵃ	*44.24*, 47.25	50.86, 57.49	49.04, 53.11	40.74, 41.96	n.m., 48.25	47.40, n.m.
L³ᵇ	46.26ᵇ	*45.50*ᶜ		40.01ᵇ	*39.52*ᶜ	
nota	33.31	d	*32.15*	30.88	d	*30.36*
RRR-L⁷ᵃ	107.69	108.70	106.31	106.02	*96.92*	106.56
SSS-L⁷ᵃ	*104.08*	114.60	*103.91*	99.77	104.51	102.56
L⁸	139.49	112.98	*109.35*	138.55	*102.36*	107.81
RRR-L⁹	104.59	106.30	102.40	102.96	*95.18*	100.81
SSS-L⁹	*101.23*	109.90	102.57	98.11	97.70	100.32
RRS-L⁹	103.39	107.45	*102.40*	101.35	*95.93*	100.63
RSS-L⁹	*102.28*	108.65	102.43	99.75	96.79	100.47
RRR-L¹⁰	*105.08*	111.77	*105.15*	100.59	101.58	103.67
SSS-L¹⁰	107.18	109.15	107.32	104.60	*97.88*	106.56

ᵃ Values for *RRR* and *SSS* conformations on the hydroxyl oxygens, respectively. ᵇ (*SSR*)-AAB structure (see text). ᶜ (*SRR*)-ABB structure (see text). ᵈ Not possible; see text.
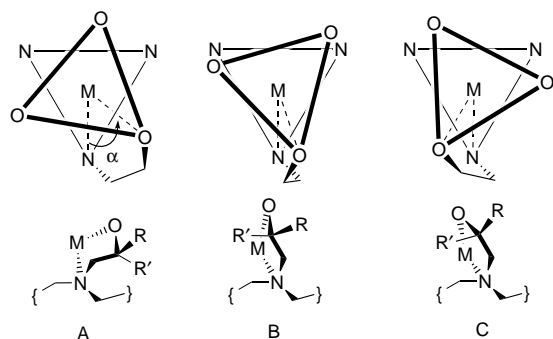
Scheme 3 Front and top views of the possible co-ordination modes of the side-chains of the metal complexes of L¹–L³ for which energy minima were observed by molecular mechanics calculations, and the resulting twist angles, α, of the plane of co-ordinating oxygens relative to the plane of macrocyclic ring nitrogens

ordination modes. Only for the sterically crowded complexes with L² and L⁸, local minima were observed for which this bond was not fully staggered. Owing to the planarity of the C-CO₂ group in nota, this acetate side-chain has one degree of freedom less, which resulted in minimized structures for modes A and C only. Table 2 shows the energies of the local minima of the complexes.

Since only the Δ conformation of the triazacyclononane ring was used in the calculations, the stereochemistry of the side-chains was varied systematically. In the complexes with L⁹ and L¹⁰ the P atoms become chiral upon co-ordination. In an analogous manner, the co-ordinating oxygens of L¹, L², L³ᵃ and L³ᵇ become chiral upon co-ordination so that also the position of the hydroxyl protons was varied systematically. For L¹, L², L³ᵃ, nota, L⁷ᵃ and L⁸, only C_3 symmetric structures were investigated.

The complexes of L³ᵃ showed the lowest energies with *R* side-chains in the B conformation and *S* side-chains in the A conformation. All C conformations had significantly higher energies. In practice, this indicates that the Mg(*SSS*-L³ᵃ) complex exists in the Δ-AAA conformation, while the corresponding calcium complex occurs as the Λ-BBB conformer. The MgL³ᵃ complex showed the lowest energy for the AAA structure (see Table 2), while for the calcium complex the BBB structure appeared to be favored. Owing to these results, we tested only the structures of ML³ᵇ in which the *R* side-chains were positioned in the B conformation and the *S* groups in the A conformation, while the hydroxyl protons were varied system-

atically. The AAA or BBB structures appeared to be not stable for these asymmetric complexes. For L³ᵇ it appeared that ABB (with the *S* side-chain in the A, and the *R* side-chain in the B conformation) was the most stable conformation for both the magnesium and the calcium complexes.

Analogously to ML³ᵃ, the symmetrical forms of ML⁹ show a preference for BBB in the Δ-*RRR* complex and for AAA in the Δ-*SSS* complex. The lower energy for the AAA form of the Δ-*SSS* complex compared to the Δ-*RRR* complex was confirmed by the crystal structures of several ML⁹ (R = Ph) complexes, which appeared to exist in the same Δ-*SSS* (or Λ-*RRR*) conformation.[12] The energy of the CCC conformations for these systems was close to the values for the AAA structures, which can be attributed to the comparable twist angles for these phosphonate side-chain containing ligands (see below). The energies of the unsymmetrical *RRS* and *RSS* forms were intermediate between the values for the *RRR* and *SSS* structures. The same appeared to be true for the complexes with L⁷ and L¹⁰, so that Table 2 only lists the extremes for the symmetrical cases. For all these ligands, BBB appeared to be the favored structure for the calcium complexes, while AAA or a combination with CCC was preferred by the magnesium complexes (see Table 2). In ML¹⁰ the apparent reversal of the energies between *RRR* and *SSS* compared to L⁷ and L⁹ is due to a change in the priorities on the phosphorus stereocenters.

In the C_3 symmetric complexes the co-ordination modes AAA, BBB and CCC give rise to different 'twist angles', α, *i.e.* the rotation of the plane of co-ordinating oxygen atoms compared to the plane of ring nitrogens (Scheme 3). Owing to the non-planarity of the macrocyclic ring (Δ/Λ conformations), these compounds contain an inherent twist of the plane of the side-chain carbon atoms directly connected to the ring nitrogens. Here, we define a positive α as a twist of the plane of co-ordinating oxygens in the same direction as that of the plane of side-chain carbons relative to the ring nitrogens. According to this definition, a trigonal prismatic structure has a twist angle of 0°, while an octahedron has α = +60° (or −60°). The twist α was large and positive for the AAA configuration, smaller (but positive) for BBB, and negative for CCC. Angles for the lowest-energy structures of the C_3-symmetrical complexes are given in Table 1. For the unsymmetrical complexes, these angles differed slightly for each side-chain, such as for ML⁷ᵇ, or the side-chains even adopted different co-ordination modes within the same complexes with concomitant large angle differences, as observed for ML³ᵇ (see below). Owing to the larger P–C and P–O bond lengths compared to C–C and C–O, respectively,

complexes of L^7–L^{10} generally showed larger twist angles, especially for the AAA and CCC structures (in BBB, both longer bonds counteract so that the effect on α is minimal).

The preferred structure appears to depend on the size of the metal ion. Crystal structures of some transition-metal complexes showed that the zinc complex of L^{3a} adopted the BBB conformation (α = 4.5°),[13] while the smaller cations Co^{III} (α = 49.8°)[14] and Cr^{III} (α = 45°)[15] preferred the AAA structure. For nota, the complexes of Ni^{II} (α = 45.0°),[16,17] Ni^{III} (α = 53.1°)[17] and Cr^{III} (α = 49.0°)[16] adopted the AAA conformation, while the larger Cu^{II} (α = −26.6°) and Fe^{III} (α = −25.2°) preferred CCC.[16] It can be easily argued that a larger twist angle provides a smaller cavity for the metal ion. Our calculations showed that particularly AAA provided a smaller cavity than either BBB or CCC. In a particular case, however, the structure of the ligand may also be the driving force for the adoption of the AAA structure as nicely demonstrated for the trimethylenetris(phenylphosphinate) derivative $L^{9'}$ (R = Ph), which adopts the AAA structure for both divalent (Co^{II}, Ni^{II}, Zn^{II} and Cu^{II}) and trivalent (Co^{III}, Fe^{III}, Ga^{III} and In^{III}) metal ions (α = 48–52°).[12]

The methyl groups in all optimized structures of L^{3a} and L^{3b} were pointing out from the center, causing all side-chains to be in the same orientation for L^{3a}, while for L^{3b} two different side-chain orientations were present in each optimized structure. This driving force seemed to favor a large twist angle for MgL^{3a} (AAA). This resulted for MgL^{3b}, however, in considerable steric hindrance between methyl groups when these had the A coordination mode. Thus, ABB appeared to provide the least steric hindrance. The absence of such a driving force, as found in MgL^1, did not result in a preference for AAA. Therefore, we concluded that a large α (AAA) is only favored when there is a driving force on the side-chains to put a residual R group away from the center and is only possible when any resulting steric hindrance between two side-chains is absent. As a result, MgL^1 adopted the BBB conformation because there is no driving force, while MgL^2 and MgL^{3b} did not adopt AAA or AAB due to resulting steric hindrance between methyl groups of neighboring side-chains. For MgL^{3a} (and for MgL^{4a} and MgL^{5a}), all factors were optimal for adopting the AAA conformation. The large twist (AAA) makes the cavity for the metal ion quite small, so that this conformation is not optimal for the larger cation Ca^{II}, which always preferred the BBB (or ABB) structure. Similar to the case of L^1, the absence of a driving force also explains the low twist angle observed for both Mg(nota) and Ca(nota), here expressed in a CCC structure since BBB is impossible (see above). This contrasts with the complexes of Ni^{II}, Ni^{III} and Cr^{III},[16,17] but in these cases the metal ion probably provides the driving force for the formation of AAA since this is closest to an octahedral arrangement.

For L^9 (R = Me) the AAA structure was favored for both the symmetrical and unsymmetrical magnesium complex. This ligand can be regarded as a structural analog of L^2 with the difference that the longer P–C and P–O bonds reduce the steric hindrance between the P=O oxygens and P–CH$_3$ groups of neighboring side-chains, so that AAA is favored in this case. Similarly, AAA is favored for MgL^{7a}, MgL^{7b} and MgL^{10}. The steric hindrance in the AAA form of MgL^8, however, is too large, similar to that observed for MgL^2. The existence of the driving force for formation of the AAA structure is clearly demonstrated for the derivative $L^{9'}$ (R = Ph),[12] as discussed above. Here, we show that a methyl group in L^{3a} and L^9 is enough for adoption of the AAA structure in the corresponding magnesium complexes. Also, both present calculations and earlier NMR data[5] on L^9 suggest that Mg^{II}/Ca^{II} selectivities are large for both the symmetrical and unsymmetrical complexes, whereas for larger R groups only the symmetrical one exists, both in the solid state ($ML^{9'}$, for various M^{II} and M^{III}, see above)[12] and in solution (MgL^{10}, see above).

As becomes apparent from Table 1, a ligand showed a large
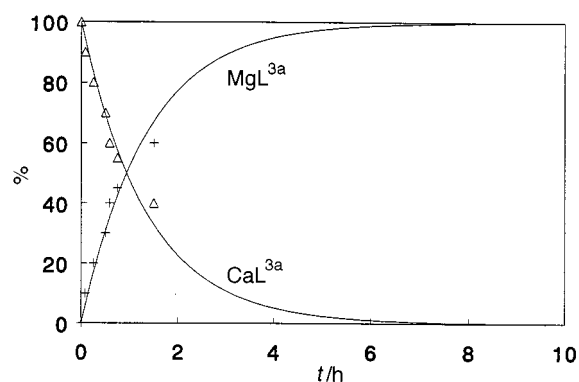
Fig. 2 Relative concentrations of the MgL^{3a} and CaL^{3a} *versus* time upon the addition of 1.5 equivalents of $Mg(ClO_4)_2$ to a solution of CaL^{3a} (with a 0.5 equivalent excess of Ca^{II}), measured by ^{13}C NMR spectroscopy in CD_3CN at 25 °C
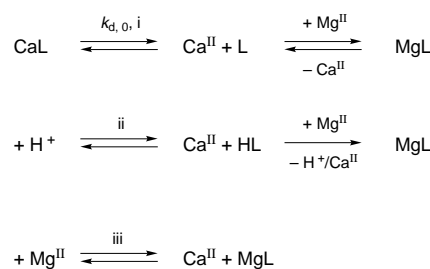
Scheme 4

Mg^{II}/Ca^{II} selectivity when a large twist angle structure, AAA, was favored for its magnesium complex. For the phosphonate side-chain containing ligands L^7, L^9 and L^{10}, also the CCC structure had a relatively small cavity (large negative α) resulting in almost equal energies and, therefore, possible contributions to the equilibrating structures in solution. Only when large twist angle structures were favored, the cavity of the ligand was significantly smaller than for the calcium complex, thus favoring the formation of the magnesium complex. The forces that govern whether a magnesium complex adopts the AAA structure or not depend upon the nature of the side-chains, and appear to constitute a delicate balance: the different orientation of a single methyl group in L^{3a} and L^{3b} causes MgL^{3a} to favor the small cavity structure AAA, while the steric hindrance between the side-chains in the analogous structure for MgL^{3b} is too large. This resulted in a Mg^{II}/Ca^{II} selectivity difference of a factor of 2000.

Dissociation rates of the complexes

Upon addition of Mg^{II} to a solution of CaL^{3a} in CD_3CN (see above), equilibration to MgL^{3a} took place over a period of several hours (see Fig. 2). In this process the dissociation of CaL^{3a} is the rate-determining step since the formation of MgL^{3a} is very rapid, as observed for the addition of Mg^{II} to free L^{3a} by which MgL^{3a} is formed instantaneously. The dissociation of CaL^{3a} can be either (i) spontaneous, (ii) H^+ catalysed or (iii) Mg^{II} catalysed (see Scheme 4). Pathway (ii) has been observed for aqueous systems,[18] but cannot occur under the aprotic conditions employed here. Since the concentration decrease of CaL^{3a} could be fitted with a simple exponential decay curve even though the concentration of free Mg^{II} changed considerably, pathway (iii) was also ruled out. Therefore, we concluded that the dissociation rate of CaL^{3a} was determined entirely by its spontaneous dissociation [pathway (i)]. From Fig. 2, a dissociation half-time, $t_{\frac{1}{2}}$, of about 1 h was deduced ($k_{d,0} = 2.1 \times 10^{-4}$ s^{-1}).

Similar, slow behavior was observed for the equilibration of L^1–L^6 and L^{10} in the presence of an excess of Mg^{II} and Ca^{II}. The dissociation of CaL was generally somewhat faster than of the

corresponding magnesium complex. For example, for the dissociation of MgL^{3b} $t_{\frac{1}{2}} \approx 5$ h. Although the dissociation of the magnesium complexes forming the AAA structure was difficult to study due to their high stability relative to the corresponding calcium complexes, their dissociation rates did not differ dramatically as witnessed by the equilibration of $Mg^{II}/Ca^{II}/L^{3a}$ in large excess of Ca^{II} (Fig. 1, top) which was complete in about 20 h. The equilibration of L^7 and L^8 was instantaneous ($t_{\frac{1}{2}} < 1$ min), probably due to their smaller complex stabilities.

In order to investigate whether these compounds might have a potential use as ionophores in Mg^{II}-selective electrodes, we studied the dissociation rate of the magnesium complexes of L^5 and L^8 in a two-phase system. The complex of L^8 was prepared in $CDCl_3$ and brought into contact with a buffered aqueous phase containing an equal amount of edta to scavenge aqueous free Mg^{II}. Vigorous stirring was applied, and ^{13}C NMR spectra of the aqueous phase showed the formation of Mg(edta). As expected, all Mg^{II} appeared to be released from MgL^8 in the organic phase within 5 min. For L^5 (1:3 mixture of L^{5a} and L^{5b}), however, 50% of the bound Mg^{II} was released after 5 min and complete dissociation was observed only after 30 min. This led to the conclusion that the dissociation of MgL^5 is about 100 times faster in the two-phase system than in organic solvent alone. This rate is actually about the same as the dissociation rate of MgL^9 in water as studied extensively before.[18] Therefore, we believe that in the dissociation experiment in the two-phase system the polar ring unit with the Mg^{II} is positioned at the phase boundary while the long alkyl chains remain in the organic phase.

Conclusion

We have found that 1,4,7-triazacyclononane derivatives that are able to accommodate Mg^{II} in a small, tight cavity (large α) form complexes with structures (AAA) different from those of Ca^{II} (BBB). This structural difference appears to be the origin of the large Mg^{II}/Ca^{II} selectivity seen for these ligands. The forces that govern whether a magnesium complex favors the adoption of the AAA structure or not appeared to be quite delicate, since the different position of a single methyl group causes the selectivity to reverse when comparing L^{3a} and L^{3b}. In general, AAA is favored only when the residual R groups are all positioned out of the center, where steric hindrance between the side-chains is minimal. Noteworthy is also that nota, originally presented as a ligand with a (relatively) high selectivity for Mg^{II},[2] now appears to be less selective than many other [9]aneN$_3$ derivatives. This can be attributed to the preference for the small-twist-angle structure (CCC) for Mg(nota).

From the two-phase system dissociation rates it becomes clear that the performance of [9]aneN$_3$ derivatives in electrode membranes will depend on the position and rates of three equilibria: (i) the equilibrium between the magnesium complex in the bulk organic phase and the phase boundary (with the polar ring unit sticking into the aqueous phase); (ii) the release of Mg^{II} from the ring unit into the aqueous phase; (iii) the equilibrium between the free ligand in the bulk organic phase and the phase boundary. Especially (i) and (ii) lie far to the right for derivative L^5. Future research will focus on mixed side-chain derivatives, likely with two phosphonate monoester side-chains and one 2-hydroxyalkyl so that the magnesium complex is uncharged, thus facilitating accommodation in the organic phase.

References

1 A. E. Martell, R. M. Smith and R. J. Motekaitis, NIST Critical Stability Constants of Metal Complexes Database, NIST Standard Reference Database 46, NIST Standard Reference Data, Gaithersburg, MD, 1993.
2 M. J. van der Merwe, J. C. A. Boeyens and R. D. Hancock, *Inorg. Chem.*, 1985, **24**, 1208.
3 R. Ramasamy, I. Lazar, E. Brücher, A. D. Sherry and C. R. Malloy, *FEBS Lett.*, 1991, **280**, 121.
4 J. van Haveren, L. DeLeon, R. Ramasamy, J. van Westrenen and A. D. Sherry, *NMR Biomed.*, 1995, **8**, 197.
5 J. Huskens and A. D. Sherry, *J. Am. Chem. Soc.*, 1996, **118**, 4396.
6 A. Bevilacqua, R. I. Gelb, W. B. Hebard and L. J. Zompa, *Inorg. Chem.*, 1987, **26**, 2699.
7 J. Huskens and A. D. Sherry, *Chem. Commun.*, 1997, 845.
8 B. A. Sayer, J. P. Michael and R. D. Hancock, *Inorg. Chim. Acta*, 1983, **77**, L63.
9 J. Robb and R. D. Peacock, *Inorg. Chim. Acta*, 1986, **121**, L15.
10 J. H. Forsberg, R. M. Delaney, Q. Zhao, G. Harakas and R. Chandran, *Inorg. Chem.*, 1995, **34**, 3705.
11 H. Tsukube, H. Adachi and S. Morosawa, *J. Chem. Soc., Perkin Trans. 1*, 1989, 1537; *J. Org. Chem.*, 1991, **56**, 7102.
12 E. Cole, R. C. B. Copley, J. A. K. Howard, D. Parker, G. Ferguson, J. F. Gallagher, B. Kaitner, A. Harrison and L. Royle, *J. Chem. Soc., Dalton Trans.*, 1994, 1619.
13 I. Fallis, L. J. Farrugia, N. M. Macdonald and R. D. Peacock, *Inorg. Chem.*, 1993, **32**, 779.
14 A. A. Belal, L. J. Farrugia, R. D. Peacock and J. Robb, *J. Chem. Soc., Dalton Trans.*, 1989, 931.
15 L. J. Farrugia, N. M. Macdonald, R. D. Peacock and J. Robb, *Polyhedron*, 1995, **4**, 541.
16 K. Wieghardt, U. Bossek, P. Chaudhuri, W. Herrmann, B. C. Menke and J. Weiss, *Inorg. Chem.*, 1982, **21**, 4308.
17 M. J. van der Merwe, J. C. A. Boeyens and R. D. Hancock, *Inorg. Chem.*, 1983, **22**, 3490.
18 J. Huskens and A. D. Sherry, *Inorg. Chem.*, 1996, **35**, 5137.